Commensurability Effects in Superconducting Nb Films with Quasiperiodic Pinning Arrays

M. Kemmler,[1] C. Gürlich,[1] A. Sterck,[1] H. Pöhler,[1] M. Neuhaus,[2] M. Siegel,[2] R. Kleiner,[1] and D. Koelle[1,*]

[1]*Physikalisches Institut-Experimentalphysik II, Universität Tübingen, Auf der Morgenstelle 14, D-72076 Tübingen, Germany*

[2]*IMS, Universität Karlsruhe, Hertzstrasse 16, D-76187 Karlsruhe, Germany*

(Received 19 May 2006; published 6 October 2006)

We study experimentally the critical depinning current I_c versus applied magnetic field B in Nb thin films which contain 2D arrays of circular antidots placed on the nodes of quasiperiodic (QP) fivefold Penrose lattices. Close to the transition temperature T_c we observe matching of the vortex lattice with the QP pinning array, confirming essential features in the $I_c(B)$ patterns as predicted by Misko *et al.* [Phys. Rev. Lett. **95**, 177007 (2005)]. We find a significant enhancement in $I_c(B)$ for QP pinning arrays in comparison to I_c in samples with randomly distributed antidots or no antidots.

DOI: 10.1103/PhysRevLett.97.147003 PACS numbers: 74.25.Qt, 74.25.Sv, 74.70.Ad, 74.78.Na

The formation of Abrikosov vortices in the mixed state of type-II superconductors [1] and their arrangement in various types of ''vortex phases'', ranging from the ordered, triangular Abrikosov lattice to disordered phases [2–4] has a strong impact on the electric properties of superconductors. Both in terms of device applications and with respect to the fundamental physical properties of so-called ''vortex matter'', the interaction of vortices with defects, which act as pinning sites, plays an important role. Recent progress in the fabrication of nanostructures provided the possibility to realize superconducting thin films which contain artificial defects as pinning sites with well-defined size, geometry, and spatial arrangement. In particular, artificially produced *periodic arrays* of submicron holes (antidots) [5–8] and magnetic dots [9–12] as pinning sites have been intensively investigated during the last years, to address the fundamental question how vortex pinning—and thus the critical current density j_c in superconductors—can be drastically increased.

In this context, it has been shown that a very stable vortex configuration, and hence an enhancement of the critical current I_c occurs when the vortex lattice is commensurate with the underlying periodic pinning array. This situation occurs, in particular, at the so-called first matching field $B_1 = \Phi_0/A$, i.e., when the applied field B corresponds to one flux quantum $\Phi_0 = h/2e$ per unit-cell area A of the pinning array. In general, $I_c(B)$ may show a strongly nonmonotonic behavior, with local maxima at matching fields $B_m = mB_1$ (m: integer or a rational number), which reflects the periodicity of the array of artificial pinning sites.

As pointed out by Misko *et al.* [13], an enhancement of I_c occurs only for an applied field close to matching fields, which makes it desirable to use artificial pinning arrays with many built-in periods, in order to provide either very many peaks in $I_c(B)$ or an extremely broad peak in $I_c(B)$. Accordingly, Misko *et al.* studied analytically and by numerical simulation vortex pinning by quasiperiodic chains and by 2D pinning arrays, the latter forming a fivefold Penrose lattice [14], and they predicted that a Penrose lattice of pinning sites can provide an enormous enhancement of I_c, even compared to triangular and random pinning arrays.

We note that the discovery of quasicrystals [15] has, until today, stimulated intensive investigations of a large variety of artificially generated quasiperiodic systems, such as semiconductor heterostructures [16], optical superlattices [17], photonic quasicrystals [18], atoms in optical potentials [19], superconducting wire networks [20], and Josephson junction arrays [21]. The investigation of the static and dynamic properties of *vortex quasicrystals*, including phase transitions which may be tuned by temperature and magnetic field, is interesting, both from a practical point of view (regarding controllability and enhancement of critical currents in superconductors) and also with respect to our understanding of fundamental aspects related to the physics of quasicrystals.

Here, we present results on the experimental investigation of matching effects in superconducting Nb thin films containing various types of antidot configurations. We studied $I_c(B)$ at variable temperature T close to the superconducting transition temperature T_c, and we compare Penrose lattices with triangular lattices, with random arrangements of antidots and with thin films without antidots. Our experimental results on Penrose arrays confirm essential features in the $I_c(B)$ patterns as predicted in [13].

The experiments were carried out on $d = 60$ nm thick Nb films which were deposited by dc magnetron sputtering in the same run on five separate substrates. Patterning was performed by e-beam lithography and lift-off to produce cross-shaped Nb bridges with circular antidots arranged in different geometries. Figure 1(a) shows the geometry of the Nb bridges, with segments of width $w = 200$ μm and length (separation between voltage pads) $l = 600$ μm. On each chip we are able to directly compare eight different cross structures. Six of them contain approximately $N_p = 110\,000$ circular antidots with radius $r = 125$ or 200 nm, arranged in either a triangular lattice [Fig. 1(b)], a Penrose lattice [Fig. 1(c)], or in a random arrangement [Fig. 1(d)]. All samples have the same average antidot

density $n_p = 0.52\ \mu\mathrm{m}^{-2}$, which corresponds to a first matching field $B_1 = n_p\Phi_0 = 1.08$ mT. For reference measurements each chip also contains two cross structures without antidots (''plain'' sample).

The fivefold Penrose lattice consists of two types of rhombuses with equal sides $a_P = 1.54\ \mu$m: ''large'' and ''small'' ones, with angles $(2\Theta, 3\Theta)$ and $(\Theta, 4\Theta)$, respectively, $(\Theta = 36°)$. Accordingly, the short diagonal of the small rhombuses $a_P/\tau = 0.952\ \mu$m; $\tau = (1+\sqrt{5})/2 \approx 1.618$ is the golden mean. The rhombuses have been arranged using inflation rules [14] in order to assure the quasiperiodicity of the lattice. In the triangular lattice the next-neighbor distance is $a_T = 1.49\ \mu$m. For the random arrangement of antidots their (x, y) coordinates were generated by a 2D array filled with uniform random numbers and then scaled to give $n_p = 0.52\ \mu\mathrm{m}^{-2}$.

To characterize our devices, we measured resistance R vs T (at $B = 0$) and determined T_c of the different bridges on each chip. The left inset in Fig. 2(a) shows $R(T)$ curves for perforated bridges and for one bridge without antidots on chip #2. For the perforated bridges, $T_c = 8.660$ K is reduced by 12 mK compared to the bridge without antidots. This can be attributed to a small contamination from the resist structure during Nb film deposition, as we observed a similar behavior on other chips. The perforated bridges also show a larger normal resistance, which can be ascribed to geometry effects and to a slight reduction in the mean free path l as compared to the plain bridge; again, this is consistently observed for all chips. With this respect, the $R(T)$ curves shown in the left inset of Fig. 2(a) are representative for all devices on various chips which we investigated. From the measured resistivity $\rho_{10\ \mathrm{K}} = 5.52\ \mu\Omega$cm of the plain film at $T = 10$ K and the relation $\rho l = 3.72 \times 10^{-6}\ \mu\Omega\mathrm{cm}^2$ [22] we estimate $l \approx 6$ nm. In total we investigated 12 bridges on three different chips (#1, #2, #3). Below we present data for bridges with $r = 200$ nm antidots on chips #2 and #3. Bridges with $r = 125$ nm antidots on chip #1 behaved similarly.

Figure 3 shows $I_c(B)$ patterns of a Penrose array at three different temperatures close to T_c. Here, I_c is defined by a dynamic criterion, i.e., via the detection of a threshold voltage $V_c = 1\ \mu$V and the T stability is ≈ 1 mK. For comparison, we insert the calculated $I_c(B)$ dependence (as the dashed line), replotted from Fig. 2(e) in [13] (for $N_p = 301$ pinning sites), without any adjustable parameter. For

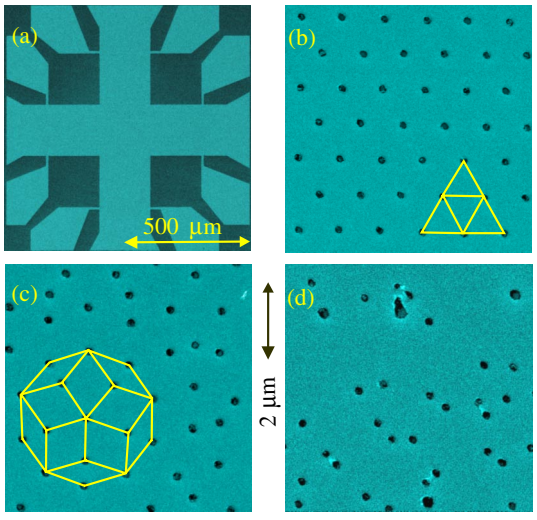

FIG. 1 (color online). Images of (a) cross-shaped Nb bridge and of different arrangements of antidots (125 nm radius): triangular lattice (b), Penrose lattice (c), random arrangement (d). The lines in (b),(c) illustrate the lattice geometries.

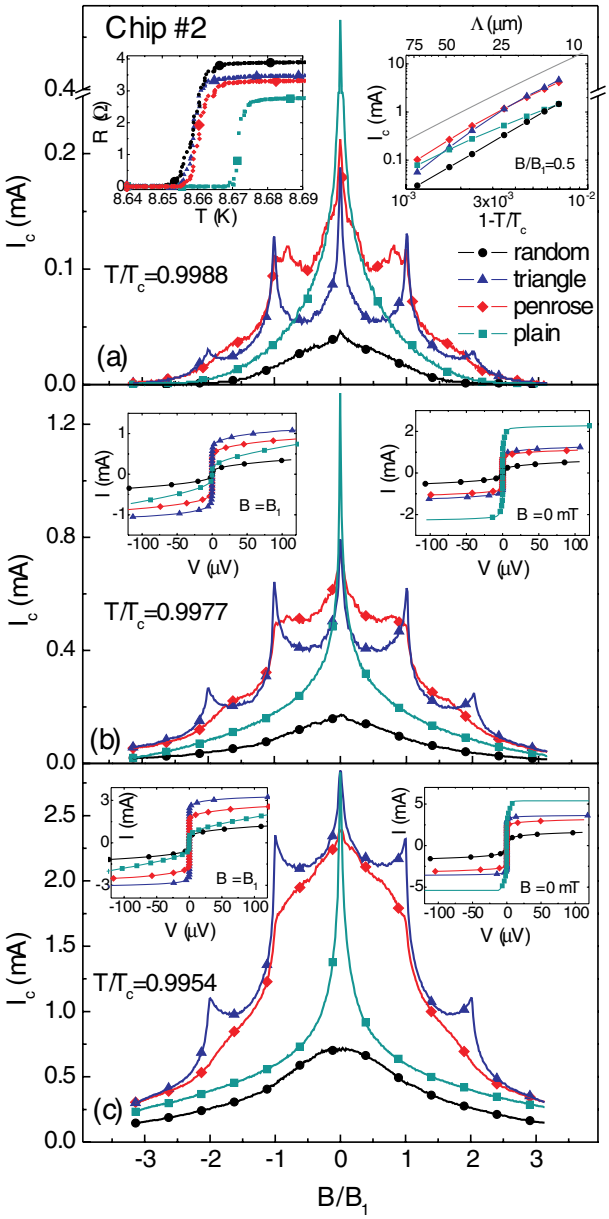

FIG. 2 (color online). Comparison of four different bridges (chip #2, $r = 200$ nm). Main graphs: I_c vs B ($V_c = 2\ \mu$V); T decreases from (a) to (c). Insets in (a): R vs T at $B = 0$, $I = 10\ \mu$A (left) and I_c vs $(1 - T/T_c)$ at $B = B_1/2$ (right); gray solid line is calculated with a simple core pinning model. Insets in (b),(c): I vs V at $B = 0$ (right) and $B = B_1$ (left).

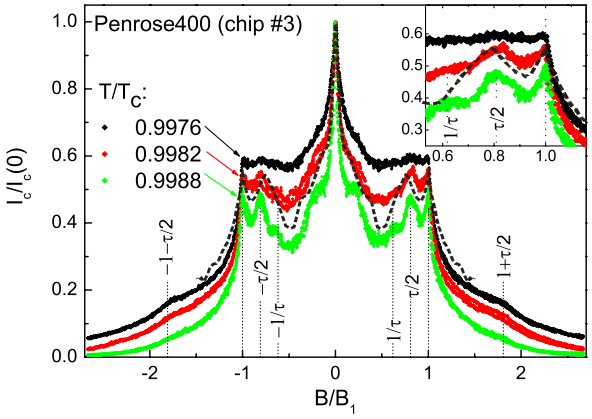

FIG. 3 (color online). I_c vs B of a Penrose array (chip #3, $r = 200$ nm, $V_c = 1$ μV) at different T close to $T_c = 8.425$ K. I_c is normalized to $I_c(B = 0) = 0.71$, 0.39, and 0.16 mA at $T/T_c = 0.9976$, 0.9982, and 0.9988, respectively. Inset shows magnification at $0.5 \lesssim B/B_1 \lesssim 1.15$. B has been swept through a full cycle (from its minimum value up to its maximum and back). Dotted lines show simulation result redrawn from Fig. 2(e) in [13] for $N_p = 301$.

these calculations a static I_c definition (number of pinned vortices over the number of vortices) was used. However, Misko *et al.* [13] mention that dynamic simulations give essentially equal results. We find very nice agreement with our experimental data for the two highest temperatures (lower and middle traces): The narrow peak in $I_c(B)$ at $B \approx 0$ broadens above $B/B_1 \approx 0.2$, until a local minimum in $I_c(B)$ is reached at $B/B_1 \approx 0.5$; a two-peak structure appears with I_c maxima at $B/B_1 = 0.81 \approx \tau/2$ (broader peak) and at $B = B_1$ (narrow peak). Above B_1, I_c drops rapidly with increasing B. The two-peak structure was predicted in [13] for the case that the gain in pinning energy E_{pin} exceeds the increase in elastic energy E_{el} associated with the deformation of a triangular vortex lattice. Misko *et al.* [13] find the broader peak at a value of $B_{v/t}/B_1 = 0.757$, which corresponds to filling of only three out of four of the pinning sites on the vertices of the small rhombuses, except for the N_d cases when two small rhombuses are connected along one side, and share one such vacancy. We find for our large Penrose arrays $N_d = N_s/\tau^2$ (N_s and N_l are the number of small and large rhombuses, respectively). With the number of vertices in the Penrose lattice $N_p = \tau N_l = \tau^2 N_s$, one obtains $B_{v/t}/B_1 = 2/\tau^2 \approx 0.764$. This is just slightly below the matching peak which we observe at $\tau/2 = (N_p - \frac{N_s}{2})/N_p$. The latter corresponds, e.g., to a vortex configuration with *every second* small rhombus having only three out of four pinning sites occupied. In addition, we find at the highest temperature $T/T_c = 0.9988$ a third peak in $I_c(B)$ at $B/B_1 = 0.65 \approx 1/\tau$, which can be associated with filling of only three out of four pinning sites on the vertices of *all* small rhombuses.

With decreasing T another peaklike structure appears at $B/B_1 = 1.77$, close to $1 + (\tau/2)$. In the same T range, the triangular array with the same antidot size (on the same chip) develops a clear peak in $I_c(B)$ at the second matching field B_2. This can be explained by an increase of the saturation number [23] $n_s \approx r/2\xi(T)$ above a value of two (ξ is the coherence length). That is, by lowering T, pinning of multiquanta occurs. The observed matching peak at $1 + (\tau/2)$ corresponds then, e.g., to double occupancy of antidots, except for one antidot on every second small rhombus, which is only occupied by a single vortex. The fact that this matching peak is not very pronounced indicates that E_{pin} only slightly exceeds E_{el}, which also explains the missing of a matching peak at $B = B_2$.

The matching peaks in Fig. 3 are most pronounced at the highest temperature, $T/T_c = 0.9988$, and gradually transform into a plateaulike $I_c(B)$ pattern (within $0.5 \leq B/B_1 \leq 1$) at $T/T_c = 0.9976$. This plateau is a remarkable feature, which we associate with the effectiveness of the many built-in periods of the Penrose lattice. We note that the Pearl length [24] $\Lambda(T) \propto (1 - T/T_c)^{-1}$, which sets the vortex interaction range, changes from ≈ 80 to 40 μm with decreasing T in Fig. 3. In contrast to the calculations in [13], with a penetration depth of the order of the pinning lattice spacing a, we find distinct matching peaks only for $\Lambda \gg a$, i.e., if the vortices interact over a large fraction of the Penrose array. Certainly, a better understanding of our results requires a more detailed theoretical analysis, including the T dependence of the vortex interaction range, pinning strength, and pinning range, as well as thermal fluctuations which might be important, in particular, close to T_c.

For direct comparison, we simultaneously measured on a single chip (#2) three perforated bridges with different antidot configurations (Penrose, triangular, and random; $r = 200$ nm) and one plain bridge. Figure 2 shows $I_c(B)$ at three different values of T/T_c. In contrast to the plain and "random" samples the Penrose and triangular arrays show clear matching effects, with identical B_1, as designed. The triangular array shows very pronounced matching peaks at B_1 and B_2. We do not observe higher order matching peaks, which indicates that $n_s \approx 2$.

The $I_c(B)$ pattern for the Penrose array is very similar to the one on chip #3 with the same antidot size (cf. Fig. 3). Decreasing T, the multiple peak structure at $B \leq B_1$ turns into a broad shoulder. When T is lowered further [see Fig. 2(c)], the shoulder transforms into a domelike structure. We cannot give a concise explanation for the shape of this very broad central peak; however, we note that we observed this on all investigated Penrose arrays.

Comparing absolute values of I_c for the Penrose and triangular array shows that very close to T_c critical currents at $B = 0$, B_1 and B_2 are quite similar; however, due to the stronger reduction in I_c of the triangular array between matching fields, the Penrose array is superior, in particular, for small fields, below B_1 [see Fig. 2(a)]. This situation changes with decreasing T, as the reduction in I_c of the triangular array between matching fields becomes much

less pronounced [see Fig. 2(c)]. That is, we cannot confirm the prediction [13] that the Penrose lattice provides an enormous enhancement in $I_c(B)$ over the triangular one, except for T very close to T_c and fields between $B = 0$ and the first matching field. This is also visible in the right inset in Fig. 2(a), which shows $I_c(1 - \frac{T}{T_c})$ at $B = 0.5B_1$ for all four samples. Above $1 - \frac{T}{T_c} \approx 3 \times 10^{-3}$ the Penrose and triangular array show almost the same $I_c(T)$ which approaches, within a factor of 2, the Ginzburg-Landau depairing current $I_{dp} \propto H_c^2 \xi \propto (1 - \frac{T}{T_c})^{3/2}$, with the thermodynamic critical field H_c. This scaling can be derived within a simple core pinning model, neglecting vortex-vortex interactions. The resulting $I_c(T)$—shown as a gray line in the right inset in Fig. 2(a)—is then simply determined by the maximum pinning force of an antidot, which we calculated, following the approach in [3] based on the London approximation [23]. The random sample gives always significantly smaller I_c as the triangular and Penrose arrays. However, it shows a steeper $I_c(T)$ dependence, which scales as $(1 - \frac{T}{T_c})^q$ over the investigated range of T, with an increase in q from $q = 2$ at $B = 0$ to $q = 2.2$ at $B = 0.5B_1$ to $q = 2.4$ at $B = B_1$. This behavior cannot be explained within our simple model and certainly deserves further investigations.

Finally, we note that the choice of the voltage criterion V_c for determining I_c does not significantly affect the shape of the $I_c(B)$ curves; we checked this for various samples and V_c ranging from 10 nV to 10 μV. For a more detailed analysis, we measured current voltage characteristics (IVCs) as shown in the insets of Figs. 2(b) and 2(c) for all four bridges at $T/T_c = 0.9977$ and 0.9954, respectively. The IVCs of the perforated bridges evolve smoothly into the resistive state. In particular, there is no sudden change in differential resistance R_d pointing to a sudden increase of the number of moving vortices. At $B = 0$ (right-hand insets) the IVCs of the different bridges do not cross (this holds up to at least 1 mV). Such a crossing is, however, observed in finite fields. As shown in the left-hand insets ($B = B_1$), R_d of the plain bridge is smaller than for the other bridges. At $V \approx 300$ μV its IVC intersects those of the triangular and Penrose arrays. A similar crossing is also observed for other values of field and temperatures, however, always well above the threshold voltage V_c used for determining I_c.

In conclusion, we experimentally verified theoretical predictions of the main features of the critical current dependence on the applied magnetic field in a superconducting thin film with a quasiperiodic Penrose lattice of antidots at temperatures close to T_c. In particular, we found matching of the vortex lattice with the quasiperiodic lattice of pinning sites very close to T_c, and we associate various matching peaks in $I_c(B)$ with distinct regular arrangements of the vortices. In addition, we directly compared different arrangements of artificial pinning sites in our Nb films. We find an enhancement of I_c in films with Penrose lattices as compared to films with random arrangement of pinning sites and films without artificial pinning sites, however, no significant enhancement of I_c as compared to films with triangular antidot lattices. With respect to applications, it will be interesting to perform more detailed investigations on the effect of optimum antidot size (i.e., saturation number) and density over a wide range of temperatures in quasiperiodic pinning arrays.

We thank Eric Sassier for his support on the measurement setup, and we gratefully acknowledge helpful discussions with V. Misko, F. Nori, and A. V. Silhanek. This work was supported by the Deutsche Forschungsgemeinschaft (DFG; Nos. KL-930/10 and SFB/TR21). M. Kemmler gratefully acknowledges support from the Evangelisches Studienwerk e.V. Villigst.

Note added.—After first submission of our manuscript we learned about related work by Villegas *et al.* [25] and Silhanek *et al.* [26] on quasiperiodic pinning arrays in superconducting films with magnetic dots.

*Electronic address: koelle@uni-tuebingen.de

[1] A. A. Abrikosov, Sov. Phys. JETP **5**, 1174 (1957).
[2] D. R. Nelson and V. M. Vinokur, Phys. Rev. B **48**, 13 060 (1993).
[3] G. Blatter *et al.*, Rev. Mod. Phys. **66**, 1125 (1994).
[4] E. H. Brandt, Rep. Prog. Phys. **58**, 1465 (1995).
[5] M. Baert *et al.*, Phys. Rev. Lett. **74**, 3269 (1995).
[6] V. V. Moshchalkov *et al.*, Phys. Rev. B **57**, 3615 (1998).
[7] A. Castellanos *et al.*, Appl. Phys. Lett. **71**, 962 (1997).
[8] K. Harada *et al.*, Science **274**, 1167 (1996).
[9] J. I. Martin *et al.*, Phys. Rev. Lett. **79**, 1929 (1997).
[10] D. J. Morgan and J. B. Ketterson, Phys. Rev. Lett. **80**, 3614 (1998).
[11] M. J. Van Bael *et al.*, Phys. Rev. B **59**, 14 674 (1999).
[12] J. E. Villegas *et al.*, Phys. Rev. B **68**, 224504 (2003).
[13] V. Misko, S. Savel'ev, and F. Nori, Phys. Rev. Lett. **95**, 177007 (2005); see also Phys. Rev. B **74**, 024522 (2006).
[14] *Quasicrystals*, edited by J.-B. Suck, M. Schreiber, and P. Häussler (Springer, Berlin, 2002).
[15] D. Shechtman *et al.*, Phys. Rev. Lett. **53**, 1951 (1984).
[16] R. Merlin *et al.*, Phys. Rev. Lett. **55**, 1768 (1985).
[17] S.-N. Zhu, Y.-Y. Zhu, and N.-B. Ming, Science **278**, 843 (1997).
[18] M. Notomi *et al.*, Phys. Rev. Lett. **92**, 123906 (2004).
[19] L. Guidoni *et al.*, Phys. Rev. Lett. **79**, 3363 (1997).
[20] A. Behrooz *et al.*, Phys. Rev. Lett. **57**, 368 (1986).
[21] K. N. Springer and D. J. V. Harlingen, Phys. Rev. B **36**, 7273 (1987).
[22] A. F. Mayadas, R. B. Laibowitz, and J. J. Cuomo, J. Appl. Phys. **43**, 1287 (1972).
[23] G. S. Mkrtchyan and V. V. Schmidt, Sov. Phys. JETP **34**, 195 (1972).
[24] J. Pearl, Appl. Phys. Lett. **5**, 65 (1964).
[25] J. E. Villegas *et al.*, Phys. Rev. Lett. **97**, 027002 (2006).
[26] A. V. Silhanek *et al.* (unpublished).